International Journal of Fatigue 47 (2013) 292–299

Contents lists available at SciVerse ScienceDirect

International Journal of Fatigue

journal homepage: www.elsevier.com/locate/ijfatigue

Effects of laser peening with different coverage areas on fatigue crack growth properties of 6061-T6 aluminum alloy

S. Huang [a,b,*], J.Z. Zhou [a], J. Sheng [a], K.Y. Luo [a], J.Z. Lu [a], Z.C. Xu [a], X.K. Meng [a], L. Dai [a], L.D. Zuo [a], H.Y. Ruan [a,b], H.S. Chen [a]

[a] School of Mechanical Engineering, Jiangsu University, Zhenjiang 212013, PR China
[b] V-zenith Laser Technology Company, Zhenjiang 212013, PR China

ARTICLE INFO

Article history:
Received 17 June 2012
Received in revised form 16 September 2012
Accepted 18 September 2012
Available online 28 September 2012

Keywords:
Laser peening
Fatigue crack growth rate
Fracture
Fatigue striation
Coverage area

ABSTRACT

The effects of coverage area on fatigue crack growth (FCG) properties of 6061-T6 aluminum alloy subject to multiple laser peening (LP) impacts were investigated. Residual stress, micro-structure and fatigue striation pattern on fracture cross-sections were analyzed. Compressive residual stresses and dense dislocation arrangements can be found in the superficial layer after LP. LP coverage area has a direct influence on FCG properties as verified by different size of shell ridges and fatigue striation spacing on fracture cross-sections. Meanwhile, FCG rate decreases with the increase of compressive residual stresses distribution perpendicular to the crack growth direction in the initial FCG stage.

1. Introduction

Fatigue crack growth (FCG) behaviors of aluminum (Al) alloys are of great technological importance for ensuring fail-safe material design in engineering applications [1,2]. It is well-known that FCG behaviors can be impeded by compressive residual stresses but accelerated by tensile residual stresses perpendicular to the crack [3,4]. Shot peening is a conventional and widely applied process to improve FCG properties by generating compressive residual stresses in the metal surface [5,6]. In order to reduce the surface roughness and deepen the compressive residual stresses distribution, many new peening technologies such as laser peening [7], cavitation shotless peening [8], ultrasonic peening [9] and micro-shot peening [10,11] were developed. Among these peening technologies, laser peening (LP) is an emerging surface modification technology which introduces deeper compressive residual stresses and less occurrence of defects in the material surface. It can significantly improve the mechanical performance and reduce FCG rate on a number of metals [7,12–14]. Nowa's, many attentions have been paid to investigate the effects of different processing parameters on the FCG properties induced by LP [15–19].

Rubio-Gonzalez et al. examined the effects of pulse density on mechanical properties of 6061-T6 Al alloy and 2205 duplex stainless steel induced by two-sided LP, and the results indicated that FCG rate decreased while fracture toughness increased with the increased pulse density [15,16]. We observed that the distance from fatigue crack initiation (FCI) to top surface increased while fatigue striation spacing on the FCG area decreased with the increment of LP impact number on the notched 6061-T6 CT samples in the previous work [17]. The study of Yang et al. showed that LP can effectively extend the FCI life and decrease FCG rate of 2024-T3 Al alloy with various pre-existing notch configurations [18].

Most of the above researches have been focusing on the effects of LP processing parameters such as the pulse density [15,16], impact number [14,17], geometry of sample [18], as well as laser spot size [19], on surface integrity and fatigue life of alloys, but few attentions have been paid to the effects of LP coverage area on their mechanical properties and fatigue performance. Kim et al. investigated the effects of different weld coverage areas (either parallel, perpendicular or 45° to the dynamically recrystallized zone) on FCG behaviors of friction stir welded Al alloy samples, and the results showed that processing coverage area significantly affected the FCG properties [20]. We also found that FCI and FCG of 7050-T7451 Al alloy treated by four paths can more effectively be restrained than two paths during two-sided LP in the previous work [21,22]. Therefore, it is important and necessary to investigate the effects of coverage area on the FCG properties of alloys subjected to multiple LP impacts in engineering applications.

Meanwhile, more attempts have mainly been made to the strengthening effects of residual stress [14–19], fracture toughness

* Corresponding author. Address: Xuefu Road 301, Jingkou District, Zhenjiang 212013, PR China. Tel.: +86 511 88786318; fax: +86 511 88780241.
E-mail address: huangshu11@sina.com (S. Huang).

0142-1123/$ - see front matter © 2012 Elsevier Ltd. All rights reserved.
http://dx.doi.org/10.1016/j.ijfatigue.2012.09.010

Nomenclature

σ_y	yield strength of material	P	fatigue loads
σ_b	tensile strength of material	B	plate thickness
E	elastic modulus	W	plate width
v	Poisson's ratio	a	crack length
R	stress ratio	N	total number of load cycles
da/dN	fatigue crack growth rate	LP	laser peening
ΔK	stress intensity factor range	FCG	fatigue crack growth
C	paris law coefficient	FCI	fatigue crack initiation
m	Paris law exponent	SIF	stress intensity factor
K_I	stress intensity factor for mode I of crack growth		

[15,16], surface deformation [19], as well as fatigue life [14–18] of metallic materials, but the changes of dislocation arrangement in the superficial layer and fatigue striation pattern on the fracture surface induced by different LP coverage areas are still pending. In fact, the micro-structure in the superficial layer is now widely acknowledged to exert a strong influence on FCG properties [13,23,24], and the characteristic of fracture micro-structure can reflect macroscopic and microscopic performance of metallic materials [17,21,22]. Hence, it is crucial to understand the mechanism of FCG resistance induced by different LP coverage areas based on the micro-structure observation.

The aim of the present work is to examine the effects of coverage area on FCG properties of 6061-T6 Al alloy subject to multiple LP impacts. Surface residual stress along the parallel and perpendicular direction is measured. Special attentions are paid to the changes of dislocation arrangement in the superficial layer and fatigue striation spacing on the fracture cross-section. Furthermore, the improvement mechanism of FCG resistance of 6061-T6 Al alloy subjected to different LP coverage areas are revealed.

2. Experiment methods

2.1. Experimental material and sample

6061-T6 Al alloy was selected in this work with a chemical composition (wt.%) of 0.90% Mg, 0.62% Si, 0.33% Fe, 0.28% Cu, 0.17% Cr, 0.06% Mn, 0.02% Ti, 0.02% Zn. The mechanical properties were shown as follows, yield strength σ_y is 289.9 MPa, tensile strength σ_b is 328 MPa, elastic modulus E is 69.8 GPa and Possion's ratio v is 0.33. The samples used for FCG tests were CT samples as illustrated in Fig. 1. All the CT samples were processed with the loading axis parallel to the rolling direction. Before the process of LP, a fatigue pre-crack of 2.5 mm long (from notch tip) was grown on each sample by a MTS-809 servo-hydraulic system at room temperature (25 °C) in the air. The maximum external load was 3.0 kN. The load ratio was maintained at $R = 0.5$ and the frequency was 9 Hz with tensile sinusoidal form. After pre-cracking, the total length of the initial crack was 15 mm.

2.2. LP processing

A high energy shockwave was induced by a Q-switched Nd: YAG laser system at the Laser Technology Institute at Jiangsu University, operating at 5 Hz repetition-rate with a wavelength of 1064 nm, and the laser pulse energy was 5 J. The footprint of laser spot with a diameter of 3 mm was top-hat and the FWHM of the pulses was 10 ns. Table 1 shows the processing parameters in detail and Fig. 2a–c shows the coverage area as well as the swept direction of CT samples used in two-sided LP. During the process of LP, laser coverage areas of 15 mm × 15 mm (LP-1), 35 mm × 15 mm (LP-2) and 15 mm × 60 mm (LP-3) were selected. The overlapping rate between the adjacent spots along both the parallel direction and perpendicular direction was 50%. A water curtain with a thickness of 1–2 mm was used as the transparent confining layer and the professional Al foil with a thickness of 100 um was used as an absorbing layer to protect the surface of samples from thermal effects.

2.3. FCG testing

The FCG tests were performed on a MTS-809 servo-hydraulic system at the room temperature (25 °C) in the air. The maximum external load was maintained at 3.0 kN and load ratio R was 0.5. The frequency of 5 Hz with a tensile sinusoidal form was used. The whole FCG testing process was monitored using a COD silicon chuck in order to obtain the FCG properties under different cycles. Twelve samples were selected. Samples 1–3 were not treated with LP, samples 4–6, 7–9 and 10–12 were treated with LP-1, LP-2 and LP-3, respectively. The average value of three samples in each group was taken to analyze. Figs. 2d–f show the typical photos of FCG testing samples treated with different LP coverage areas.

2.4. Measurements of residual stress and micro-structure

Residual stress analyses were performed on the surface of laser peened CT samples either perpendicular or parallel to the peening direction, using X-ray diffraction method. Surface micro-structure of the untreated and laser peened samples was characterized by a JEM-2100 transmission electron microscopy (TEM) operated at a voltage of 200 kV. The fatigue fracture micro-structure was analyzed by an S-4800 field emission scanning electron microscopy (SEM) operated at a voltage of 15 kV.

3. Results and discussions

3.1. Residual stress

Fig. 3a shows the surface residual stress distribution along Path 1 (parallel direction as shown in Fig. 2). It is observed that tensile residual stress with the value of 92 MPa appears at the crack tip of untreated sample after pre-cracking, and it restores to the value of matrix (42 MPa) in the region of 7 mm away from the crack tip. However, the residual stresses are −112 MPa, −121 MPa and −118 MPa at the crack tip, and then increase to −207 MPa, −222 MPa and −216 MPa in the region of 14 mm away from the crack tip after LP-1, LP-2 and LP-3, respectively. Subsequently, with the sampling point moving away from the crack tip, compressive residual stresses induced by LP-1 and LP-3 gradually decrease and turn into tensile stresses. On the contrary, for LP-2 samples, the compressive residual stresses maintain at about −220 MPa

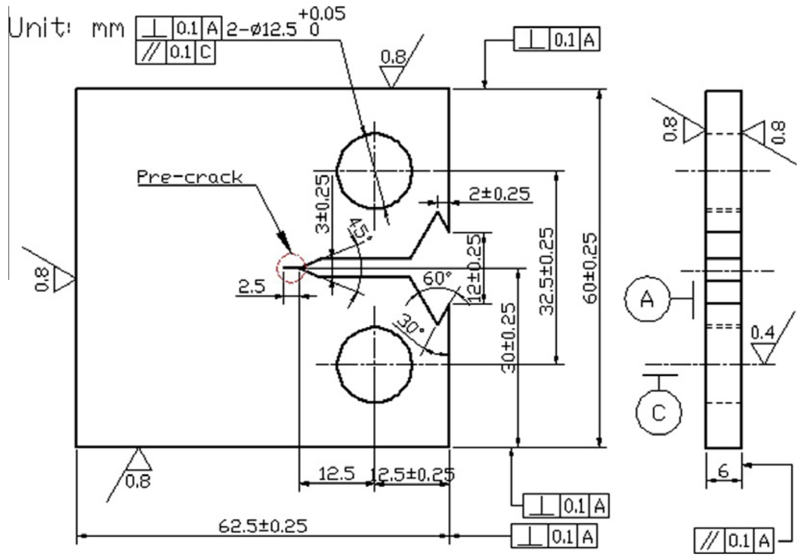

Fig. 1. Dimension of 6061-T6 compact tension samples used in the FCG tests.

Table 1
The processing parameters used in multiple LP.

Parameters	Value
Beam divergence of output (mrad)	⩽0.5
Spot diameter (mm)	3
Pulse width (ns)	10
Repetition-rate (Hz)	5
Laser wavelength (nm)	1064
Pulse energy (J)	5
Export stability	⩽±5%
Polarization	Horizontal
Beam profile	Top hat

due to the sampling point always moving inside the LP coverage area. Fig. 3b shows the surface residual stress distribution along Path 2 (perpendicular direction as shown in Fig. 2). It is observed that compressive residual stresses generate in the LP coverage area, with the maximum values of −213 MPa, −218 MPa and −225 MPa after LP-1, LP-2 and LP-3, respectively. With the sampling point moving away from the LP coverage area, compressive residual stresses induced by LP-1 and LP-2 gradually decrease and turn into tensile stresses. However, for LP-3 samples, the compressive residual stresses maintain at about −225 MPa due to the test point always moving inside the LP coverage area.

It indicates that the compressive residual stresses with a relatively uniform distribution have been generated in the LP coverage area. High amplitude compressive residual stresses can be induced by crystal defects such as high density and homogeneous dislocation, which is the main factor for greatly improving fatigue limits and dropping the fatigue gap sensitivity [13,17,24]. However, with the sampling point moving away from the LP coverage area, the compressive stresses decrease and turn into tensile state. For the notched samples, the superposition principle is often used to determine the stress intensity factor (SIF) subject to combined effects of external applied stress and residual stress [25,26]. Zhang et al. [27] introduced a weight function method to investigate the relationship between the SIF and compressive residual stresses induced by LP, and the effective SIF was used to evaluate the FCG properties. Combined with the above-mentioned experimental results, it is concluded that LP coverage area significantly affect the effective SIF along the FCG path, which have an important influence on the FCG properties.

3.2. TEM observations

Typical TEM observations of the 6061-T6 samples are shown in Fig. 4, and the test region can be found in Fig. 2b. Fig. 4a shows a TEM image in the near-surface of the untreated sample, it can be clearly seen that there are many precipitates and the dislocation density is relatively low. Figs. 4b–d show the TEM images in the near-surface of samples subjected to LP-1, LP-2 and LP-3, respectively. It is observed that the dislocation is not uniformly distributed. There are plenty of dislocation lines (as shown in Fig. 4b and c) and randomly arranged high-density dislocation tangles (as shown in Fig. 4c and d) in some grains. This phenomenon may be due to the dislocation accumulation and rearrangement for minimizing the total energy state.

Compared with the untreated samples, the dislocation lines and dislocation tangles induced by LP reveal significantly higher dislocation density, and the energy induced by highly tangled and dense dislocation arrangements would reduce the crack driving forces. Lu et al. revealed the micro-structural evolution and grain refinement mechanism of multiple LP impacts on LY2 Al alloy [24]. Combined with the above-mentioned experimental results, it is inferred that multiple LP impacts can refine the coarse grain in the superficial layer of 6061-T6 Al alloy by dislocation movement. The grain boundaries normally act as a blockage of FCG and can reduce the crack driving forces due to the energy induced by piled-up dislocations [17]. It implies that the FCG path of the untreated sample intersects the fewest grain boundaries. Furthermore, the dislocation density increases with the increase of the LP coverage area. Therefore, the FCG path of the sample subjected to LP-3 intersects the most grain boundaries in the superficial layer, and LP-3 can obtain the greatest improvement of FCG resistance.

3.3. Micro-structure on the fracture surface

Fig. 5a shows the micro-structure on fracture surface of the untreated 6061-T6 CT sample, and Fig. 5b–d shows the crack arrest and fatigue striation patterns on fracture surface of the samples subjected to LP-1, LP-2 and LP-3, respectively. From the typical photos of all the fractured CT samples, FCG paths are found basically perpendicular to the direction of external fatigue loads. From the fracture cross-section along A-A direction, it can be seen that fatigue cracks initiate at the machined notch tip and grow to

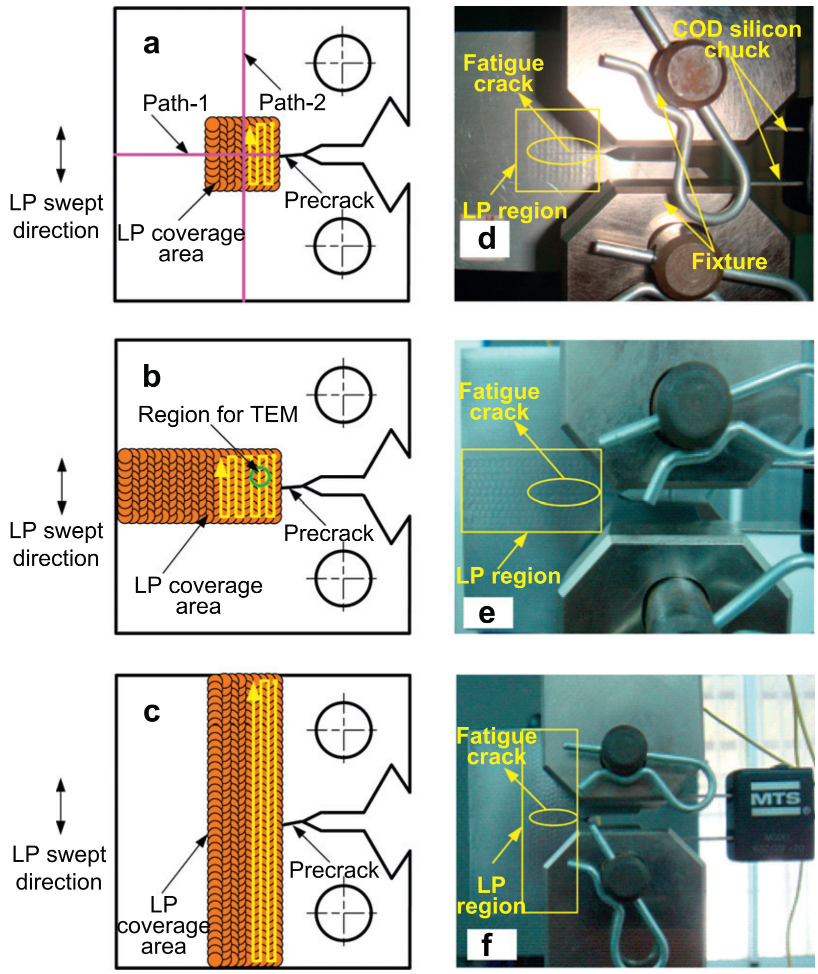

Fig. 2. Different LP coverage areas of (a) LP-1, (b) LP-2 and (c) LP-3 and typical photos of 6061-T6 CT samples used in the FCG tests of (d) LP-1, (e) LP-2 and (f) LP-3.

failure under continual fatigue cycling. Meanwhile, the whole fatigue fracture can be divided into pre-crack stage, stable FCG stage and final rupture stage. In order to study the micro-structure on stable FCG stage, the regions where appear the phenomenon of crack arrest are magnified. Compared with the untreated sample, shell ridges can be found on the fracture surface of samples subjected to LP. Figs. 5a–d also show the SEM images of fatigue striation on the crack arrest region of CT samples (a = 25 mm), it is observed that the fatigue striation spacing of the untreated sample is 0.59 μm, while it reduce to 0.32 μm, 0.23 μm and 0.12 μm after LP-1, LP-2 and LP-3, respectively.

Generally speaking, the morphology of fatigue fracture is the direct result of material progressive wreck [28]. Compared with the untreated samples, the appearance of shell ridges induced by LP signify the effects of crack arrest, which can be attributed to the compressive residual stresses and grain refinement in the superficial layers. Compared with the shell ridges of LP-1 (as shown in Fig. 5b), the shell ridges of LP-2 and LP-3 (as shown in Fig. 5c and d) are deeper and wider, which imply the better crack arrest effects. Also, it is well known that local FCG rate can be estimated from the spacing of fatigue striations observed on stable FCG stage [16,21,28]. The decrement of striations spacing indicate that LP has positive influence on fatigue properties by lowering the FCG rates compared with corresponding behavior in the untreated samples. Since the fatigue striation spacing of LP-3 is narrowest, it is inferred that the most obvious improvement of FCG resistance is obtained by LP-3.

3.4. Fatigue crack growth rate

Assuming that crack growth of untreated and laser peened CT samples is always in stable expanding stage which follows Paris formula [29]:

$$\frac{da}{dN} = C(\Delta K)^m \tag{1}$$

Stress intensity factor for mode I of crack growth K_I is determined using the following equation [30]:

$$K_I = \frac{P}{B\sqrt{W}} \frac{2 + (a/W)}{[1 - (a/W)]^{3/2}} \left[0.886 + 4.64\left(\frac{a}{W}\right) - 13.32\left(\frac{a}{W}\right)^2 + 14.72\left(\frac{a}{W}\right)^3 - 5.60\left(\frac{a}{W}\right)^4\right] \tag{2}$$

where P is external load, B and W are thickness and width of sample, a is crack length.

Fig. 6 shows the experimental curve of FCG rate da/dN as a function of SIF range ΔK, which can be regarded as linear under the logarithmic coordinates. Paris formula is adopted to fit the relationship of curves in order to obtain the constant values of C and m. The changes of C and m can be found in Table 2. Compared with the untreated samples, C decreases while m increases after LP. Meanwhile, the samples subjected to LP result in a reduction of FCG rate, and it can be indicated by the decline of $da/dN - \Delta K$ curves. The reduction is obvious in the initial FCG stage. When

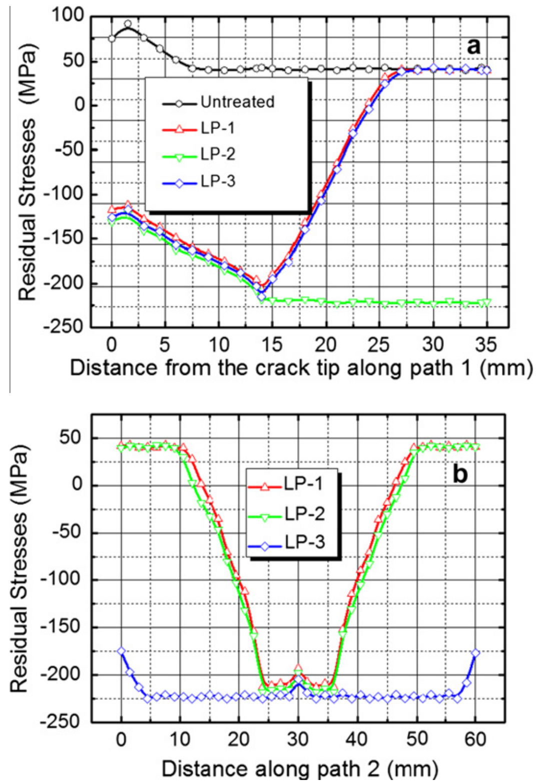

Fig. 3. Residual stresses distribution of 6061-T6 CT samples subjected to LP with different coverage areas (a) along the path 1 and (b) along the path 2.

the initial ΔK is 6.56 MPa $m^{1/2}$, da/dN is 8.09E-5 mm/cycle of the untreated sample, while the values decrease to 4.66E-5 mm/cycle, 3.80E-5 mm/cycle and 1.77E-5 mm/cycle after LP-1, LP-2 and LP-3, respectively. However, when ΔK increases to 17.81 MPa $m^{1/2}$ in the FCG final stage, the FCG rate of all the samples are almost the same.

It indicates that the improvement of FCG resistance induced by LP can be separated into a relatively large increase in the initial FCG stage and a small increase in the final FCG stage. In the initial FCG stage, compressive residual stresses induced by LP can cause the crack closure and incur the reduction of effective driving force, which is favorable for the reduction of SIF range and FCG rate [25–27]. Moreover, LP coverage area significantly affected the FCG rate in the initial FCG stage, the decrement of FCG rate induced by LP-3 is more evident than LP-1 and LP-2. It is attributed to the increase of compressive residual stresses distribution perpendicular to the crack growth direction. However, compressive residual stresses release with the increasing of crack length, and the decrement of FCG rate weakens. Even if LP-2 covers the whole path of fatigue crack, the crack arrest effects in the final FCG stage are limited, since the crack driving force is much larger than the resistance induced by compressive residual stresses.

3.5. Fatigue crack growth life

Fig. 7 shows the curves of crack length a versus cycles N on 6061-T6 CT samples subjected to LP with different coverage areas. It shows that the initial crack length of all the samples is 15 mm after pre-cracking. When the crack length increases to 32.47 mm, the untreated sample is pulled off with the final fatigue life of 80477 cycles, while the treated samples continue to expand to 33.89 mm, 34.11 mm and 34.42 mm after LP-1, LP-2 and LP-3, with the corresponding fatigue life of 100976, 115930 and 229374 cycles, respectively. Fig. 8 shows the fatigue life of 6061-T6 CT samples subjected to LP with different coverage areas.

It is obvious that fatigue life of the 6061-T6 CT samples subjected to LP is higher than that of the untreated sample at a given applied external load. The beneficial effects on the fatigue life is believed to be associated with the compressive residual stresses and dense dislocation arrangements induced by LP, which are expected to influence the FCI and FCG properties favorably. Samples subjected to LP-1, LP-2 and LP-3 respectively provide a 25.47%, 44.05% and 185.02% increment in the fatigue life as compared with the untreated sample, therefore, LP coverage area significantly affect the fatigue life. Furthermore, samples subjected to LP-3 obtain the highest fatigue life, which is due to the largest compressive residual stresses distribution in the initial stage of FCG and the most obvious grain refinement induced by highly tangled and dense dislocation arrangements.

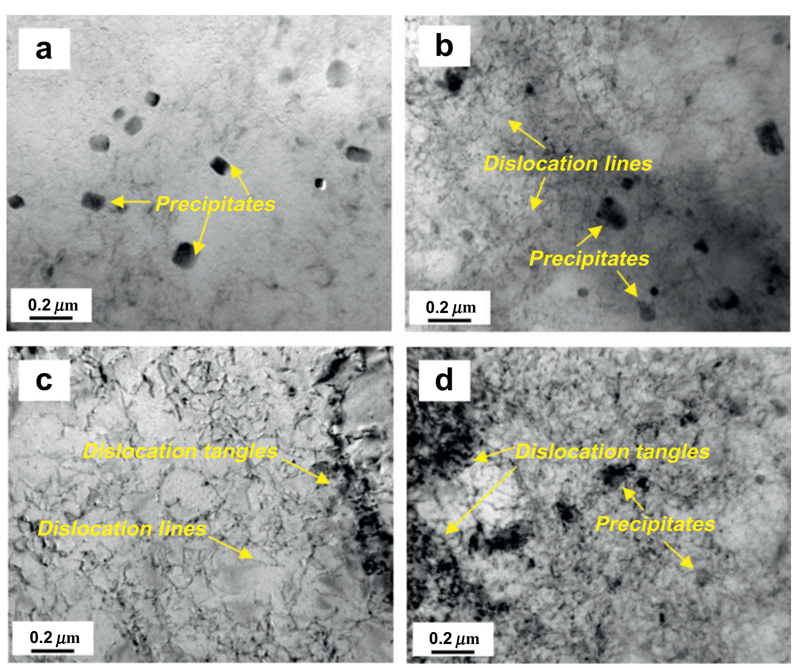

Fig. 4. Typical TEM images of 6061-T6 CT samples subjected to LP with different coverage areas (a) untreated, (b) LP-1, (c) LP-2 and (d) LP-3.

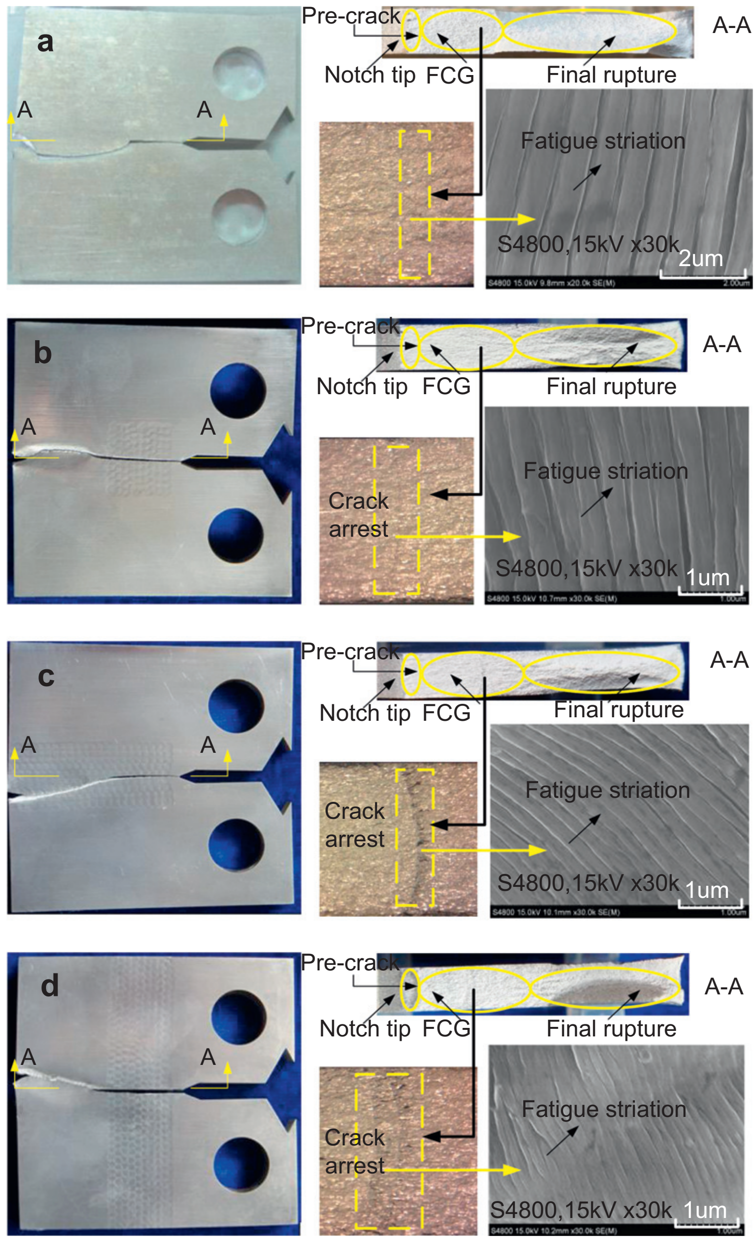

Fig. 5. Crack arrest and fatigue striation patterns on the fracture surface of 6061-T6 CT samples subjected to LP with different coverage areas (a) untreated, (b) LP-1, (c) LP-2 and (d) LP-3.

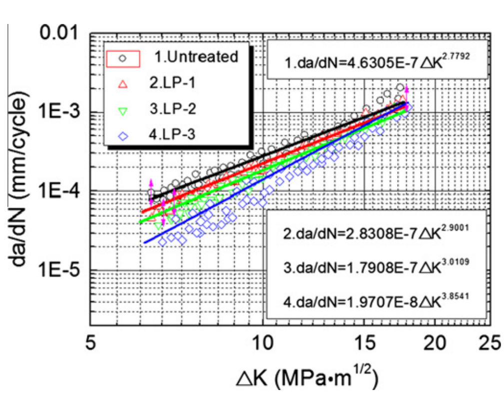

Fig. 6. FCG rate as a function of SIF range on 6061-T6 CT samples subjected to LP with different coverage areas.

Table 2
Material constants C and m of the untreated and laser peened samples.

LP way	Untreated	LP-1	LP-2	LP-3
C	4.6305E−7	2.8308E−7	1.7908E−7	1.9707E−8
m	2.7792	2.9001	3.0109	3.8541

4. Conclusions

The effects of coverage area on FCG properties of 6061-T6 CT samples subjected to multiple LP impacts were investigated. Some important conclusions have been made as follows:

(1) Compressive residual stresses with a relatively uniform distribution are generated in the LP coverage area. However, they gradually decrease and turn into tensile stresses with

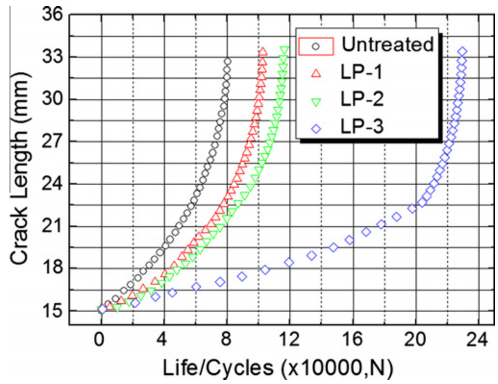

Fig. 7. Crack length as a function of FCG life on 6061-T6 CT samples subjected to LP with different coverage areas.

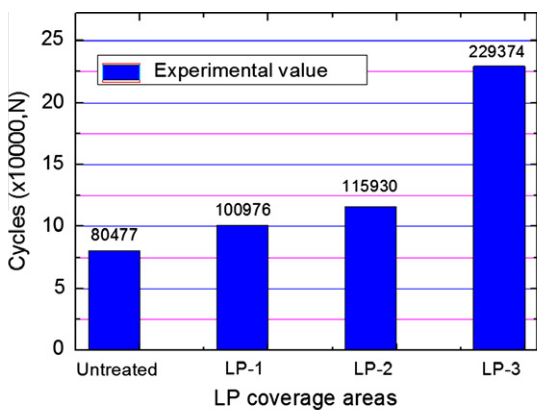

Fig. 8. Fatigue life of 6061-T6 CT samples subjected to LP with different coverage areas.

the sampling point moving away from LP coverage area. Therefore, LP coverage area can significantly affect the effective stress intensity factor along the FCG path.

(2) Highly tangled and dense dislocation arrangements can be found in the superficial surface of 6061-T6 Al alloy subjected to multiple LP impacts. The energy induced by piled-up dislocations would reduce the crack driving forces.

(3) The appearance of shell ridges and the decrement of striation spacing on the fracture surface indicate that LP has a positive influence on lowering the FCG rates compared with corresponding behavior in the untreated samples. Samples treated with LP-3 can create the most obvious FCG resistance as verified by the widest shell ridges and narrowest fatigue striation spacing.

(4) LP coverage area significantly affects the FCG rate. The decrement of FCG rate of LP-3 is more evident than LP-1 and LP-2 in the initial stage of FCG, which could be attributed to the introduction of wider compressive residual stresses distribution and more intensive dislocation arrangements. However, the reduction of FCG rate caused by LP is weak, which is due to the fact that the compressive residual stresses release with the increasing of crack length in the final stage of FCG.

Acknowledgements

The authors are grateful for the support provided by the National Natural Science Foundation of China (Nos. 51175236 and 51105179), the Natural Science Foundation of Jiangsu Province (Nos. BK2010351 and BK2011478), the Natural Science Foundation of Jiangsu Higher Education Institutions (No. 10KJB460002), Key Laboratory Foundation of Photon Manufacturing Science and Technology of Jiangsu Province (No. GZ201107) the Innovation Program of Graduated Student of Jiangsu University (No. CX09B_07XZ), the Industrial Technology Support Project of Zhenjiang (No. SGY20090026) and A Project Funded by the PAPD of Jiangsu Higher Education Institutions.

References

[1] Jones R, Molent L, Walker K. Fatigue crack growth in a diverse range of materials. Int J Fatigue 2012;40:43–50.
[2] Diana AL, Diran A. Fatigue crack growth characteristics in cast Al–Si–Mg alloys: Part II. Life predictions using fatigue crack growth data. Mater Sci Eng A 2004;385:87–199.
[3] Tran HT, Masakazu O, Kenji S. Fatigue crack propagation behavior in friction stir welding of AA6063-T5: roles of residual stress and microstructure. Int J Fatigue 2012;43:23–9.
[4] Christopher JL, Diana AL. Effects of residual stresses on fatigue crack growth behavior of structural materials: analytical corrections. Int J Fatigue 2011;33:858–67.
[5] Dalaei K, Karlsson B. Influence of shot peening on fatigue durability of normalized steel subjected to variable amplitude loading. Int J Fatigue 2012;38:75–83.
[6] Torres MAS, Voorwald HJC. An evaluation of shot peening, residual stress and stress relaxation on the fatigue life of AISI 4340 steel. Int J Fatigue 2002;24:877–86.
[7] Montross CS, Wei T, Ye L, Clark G, Mai YW. Laser shock processing and its effects on microstructure and properties of metal alloys: a review. Int J Fatigue 2002;24:1021–36.
[8] Dan O, Hitoshi S. Cavitation shotless peening for improvement of fatigue strength of carbonized steel. Int J Fatigue 2003;25:1217–22.
[9] Huo LX, Wang DP, Zhang YF. Investigation of the fatigue behaviour of the welded joints treated by TIG dressing and ultrasonic peening under variable-amplitude load. Int J Fatigue 2005;27:95–101.
[10] Kazuyuki O. Fatigue life enhancement of aluminum alloy for aircraft by fine particle shot peening (FPSP). J Mater Process Technol 2011;211:1395–9.
[11] Harada Y, Fukaura K, Haga S. Influence of microshot peening on surface layer characteristics of structural steel. J Mater Process Technol 2007;191:297–301.
[12] Hatamleh O. A comprehensive investigation on the effects of laser and shot peening on fatigue crack growth in friction stir welded AA 2195 joints. Int J Fatigue 2009;31:974–88.
[13] Lu JZ, Luo KY, Zhang YK, Sun GF, Gu YY, Zhou JZ, et al. Grain refinement mechanism of multiple laser shock processing impacts on ANSI 304 stainless steel. Acta Mater 2010;58:5354–62.
[14] Zhang XC, Zhang YK, Lu JZ, Xuan FZ, Wang ZD, Tu ST. Improvement of fatigue life of Ti-6Al-4V alloy by laser shock peening. Mater Sci Eng A 2010;527:3411–5.
[15] Rubio-Gonzalez C, Felix-Martinez C, Gomez-Rosas G, Ocana JL, Morales M, Porro JA. Effect of laser shock processing on fatigue crack growth of duplex stainless steel. Mater Sci Eng A 2011;528:914–9.
[16] Rubio-Gonzalez C, Ocana JL, Gomez-Rosas G, Molpeceres C, Paredes M, Banderas A, et al. Effect of laser shock processing on fatigue crack growth and fracture toughness of 6061–T6 aluminum alloy. Mater Sci Eng A 2004;386:291–5.
[17] Zhou JZ, Huang S, Sheng J, Lu JZ, Wang CD, Chen KM, et al. Effect of repeated impacts on mechanical properties and fatigue fracture morphologies of 6061–T6 aluminum subject to laser peening. Mater Sci Eng A 2012;539:360–8.
[18] Yang JM, Her YC, Han NL. Laser shock peening on fatigue behavior of 2024–T3 Al alloy with fastener holes and stopholes. Mater Sci Eng A 2001;298:296–9.
[19] Warren AW, Guo YB, Chen SC. Massive parallel laser shock peening: simulation, analysis, and validation. Int J Fatigue 2008;30:188–97.
[20] Kim S, Lee CG, Kim SJ. Fatigue crack propagation behavior of friction stir welded 5083-H32 and 6061-T651 aluminum alloys. Mater Sci Eng A 2008;478:56–64.
[21] Zhang L, Lu JZ, ZhangYK, Luo KY, Zhong JW, Cui CY, et al. Effects of different shocked paths on fatigue property of 7050-T7451 aluminum alloy during two-sided laser shock processing. Mater Des 2011;32:480–6.
[22] Zhang L, Luo KY, Lu JZ, Zhang YK, Dai FZ, Zhong JW. Effects of laser shock processing with different shocked paths on mechanical properties of laser welded ANSI 304 stainless steel joint. Mater Sci Eng A 2011;528:4652–7.
[23] Kwai SC. Roles of microstructure in fatigue crack initiation. Int J Fatigue 2010;32:1428–47.
[24] Lu JZ, Luo KY, Zhang YK, Cui CY, Sun GF, Zhou JZ, et al. Grain refinement of LY2 aluminum alloy induced by ultra-high plastic strain during multiple laser shock processing impacts. Acta Mater 2010;58:3984–94.
[25] Chahardehi A, Brennan FP, Steuwer A. The effect of residual stresses arising from laser shot peening on fatigue crack growth. Eng Fract Mech 2010;77:2033–9.
[26] Maawad E, Sano Y, Wagner L, Brokmeier HG, Genzel C. Investigation of laser shock peening effects on residual stress state and fatigue performance of titanium alloys. Mater Sci Eng A 2012;36:82–91.

[27] Zhang YK, Ren XD, Zhou JZ, Lu JZ, Zhou LC. Investigation of the stress intensity factor changing on the hole crack subject to laser shock processing. Mater Des 2009;30:2769–73.
[28] Ioannis B, David D, Trevor CL. The role of microtexture on the faceted fracture morphology in Ti-6Al-4V subjected to high-cycle fatigue. Acta Mater 2010;58:3908–18.
[29] Paris PC, Erdogan F. A critical analysis of crack propagation laws. J Basic Eng 1963;85(4):528–34.
[30] ASTM 2002. Annual book of ASTM standards, v. 03.01 no. E647-00. Standard test method for measurement of fatigue crack growth rates.